

Travel-Time Tomography for Local Sound Speed Reconstruction Using Average Sound Speeds

Rehman Ali
Department of Electrical Engineering
Stanford University
Stanford, CA
rali8@stanford.edu

Jeremy J. Dahl
Department of Radiology
Stanford School of Medicine
Stanford, CA
jjdahl@stanford.edu

Abstract—Our previous work on estimating the local speed of sound from average sound speed assumes a perfectly layered medium where sound speed is only allowed to vary axially away from the transducer surface. This layered-medium approach relies on inverting the relationship between the local interval sound speeds in each layer and the effective average sound speed up to a particular imaging depth. The primary limitation of this approach is that local sound speed estimation can become inaccurate in the presence of lateral variations in sound speed or a curved transducer surface. To better estimate sound speed in the presence of these non-idealities, we propose a travel-time tomographic approach that accounts for propagation paths from the scattering volume to each transducer element.

Index Terms—Speed of Sound, Ray-Tracing, Tomographic Reconstruction

I. INTRODUCTION

The sound speed in a medium fundamentally impacts how the ultrasound imaging system physically interacts with the medium being imaged. Both the travel times and signal strength of the echoes back-scattered by the medium are impacted by the speed of sound in the medium. The goal of (B-mode) ultrasound imaging is to focus the back-scattered ultrasound signal at each location in the ultrasound image by dynamically delaying-and-summing channel data at each point in the image. The delays used to focus sound at each location in the ultrasound image depend on the assumed speed of sound in the medium. If the assumed speed of sound matches the effective average speed of sound in the medium, the back-scattered signal should be coherently aligned after applying delays. However, a mismatch in the speed of sound results in a misalignment of signal after applying delays.

This signal misalignment, also known as phase aberration, not only contributes to ultrasound image degradation but can also be used to estimate speed of sound by considering the variation in sound speed along various propagation paths [1]. Some recent works have also used knowledge of the speed of sound in the medium to perform distributed phase aberration correction in diffuse scattering media [2].

Sound speed has also been used as biomarker to characterize the disease state in tissue. For example, cancer lesions can be identified as globular regions with an abnormally high speed of sound [3]. Several sound speed estimators have been proposed for the detection of cancer lesions based on sound speed

contrast using both transmission-based [3] and reflection-based [1] setups. Sound speed can also serve as a biomarker for non-alcoholic fatty liver disease (NAFLD). High fat concentration has been shown to decrease the speed of sound in the liver [4]. Many recent works [1], [2] have considered sound speed estimation in layered media in order to assess the efficacy of sound speed measurement in liver through the superficial abdominal layers. Similar models have been proposed for sound speed estimation in the liver based on focusing quality metrics and the measured thicknesses of abdominal layers [5].

Our prior work on sound speed estimation [2], [6] has been focused on estimating the local speed of sound in layered media. This work assumes infinitesimally thick layers so that as long there is negligible lateral variation in the speed of sound in the medium, the local sound speed may be estimated accurately. This model relates the effective average speed of sound up to particular depth to the local speed of sound as a function of depth. The effective average sound speed has been measured by cross-correlation [6] and coherence maximization [2]. This work introduces a new tomography-based method for sound speed estimation that directly accounts for the propagation paths between the transducer array and the scattering volume. The goal of this new tomographic approach is to better tolerate and measure the lateral variation in the speed of sound in the medium.

II. THEORY

A. Travel Times in a Spatially-Varying Sound Speed Medium

Assuming a two-dimensional medium with coordinates (x, z) and sound speed $c(x, z)$ where $(x_i, 0)$ is the location of the i th element on the transducer array, the travel time τ from the i th element to an arbitrary point (x, z) in the medium can be found using the eikonal equation

$$\sqrt{\left(\frac{\partial \tau}{\partial x}\right)^2 + \left(\frac{\partial \tau}{\partial z}\right)^2} = \frac{1}{c(x, z)} \quad (1)$$

subject to the boundary condition $\tau(x_i, 0) = 0$. The eikonal equation (12) accurately models refraction and can be solved efficiently using the fast marching method [7].

B. Model for Sound Speed in a Layered Medium

In an M -layered medium, the effective average sound speed after M layers is

$$\frac{1}{c_{avg,M}} = \frac{1}{M} \sum_{i=1}^M \frac{1}{c_i}, \quad (2)$$

where c_i is the local sound speed in the i th layer. To estimate the local sound speed in the M th layer from average sound speed estimates after the $(M - 1)$ th and M th layer, the following inversion formula can be used.

$$\frac{1}{c_M} = \frac{M}{c_{avg,M}} - \frac{M-1}{c_{avg,M-1}}. \quad (3)$$

As shown in equation (3), local sound speed estimates depends on accurate average sound speed estimates. The concept of average sound speed assumes that applying the following one-way geometric delays to focus channel data at (x_f, z_f) will align wavefronts prior to coherent summation.

$$\tau_i(x_f, z_f) = \frac{D_i(x_f, z_f)}{c_{avg}} = \frac{1}{c_{avg}} \sqrt{(x_f - x_i)^2 + z_f^2}. \quad (4)$$

C. Tomographic Reconstruction Model

Neglecting refraction and assuming that sound travels on a straight ray path from the i th transducer element at $(x_i, 0)$ to a focal point (x_f, z_f) , the travel time τ_i can be calculated as

$$\tau_i(x_f, z_f) = \int_0^{D_i(x_f, z_f)} \frac{dr}{c\left(x_i + \frac{r(x_f - x_i)}{D_i(x_f, z_f)}, \frac{rz_f}{D_i(x_f, z_f)}\right)}, \quad (5)$$

where $D_i(x_f, z_f) = \sqrt{(x_f - x_i)^2 + z_f^2}$ is the path length. By assuming that the variation in the sound speed is small enough relative to the average sound speed over the path of propagation, we can safely neglect the effects of refraction. These line integrals, indexed over all transducer elements and focal points, can be used to form a linear system of equations that relates individual pixels in the sound speed distribution of the medium to the travel time observed over each path:

$$\vec{t}_{obs} = \mathbf{H}\vec{s}, \quad (6)$$

where \vec{s} is a vector of the pixels in $\frac{1}{c(x,z)}$, \mathbf{H} is a matrix that encodes the line integrals between every pair of transducer element and focal point, and \vec{t}_{obs} is a vector of the travel times observed over those propagation paths. The average sound speed measurement at each focal point may be used to construct \vec{t}_{obs} . This linear system defines an ill-conditioned inverse problem whose goal is to recover the sound speed distribution in the medium from the measured travel times. Since phase aberration is the mechanism by which the travel times are measured, we will refer to this tomographic framework for sound speed reconstruction as inverse-modeled phase aberration computed tomography (IMPACT).

TABLE I
K-WAVE SIMULATION SETTINGS

| Parameter | Value | Units |
|----------------------|--------|----------|
| Array Geometry | Linear | - |
| Number of Elements | 128 | elements |
| Element Pitch | 0.15 | mm |
| Center Frequency | 8 | MHz |
| Fractional Bandwidth | 0.7 | - |
| Sampling Frequency | 85.56 | MHz |
| Grid Spacing | 0.03 | mm |

D. Bayesian Reformulation and Model Inversion

As part of IMPACT, we re-frame the solution of (6) as a Bayesian maximum likelihood estimation problem. First, the residuals $\vec{t}_{obs} - \mathbf{H}\vec{s}$ are modeled as a normal random variable with mean $\vec{0}$ and covariance \mathbf{R} , which is a diagonal matrix whose entries are proportional to $D_i(x_f, z_f)$. The purpose of scaling the variance of the observations with propagation distance is to account for the decrease in SNR due to attenuation and geometric spreading of the wave along the path of propagation. Second, we model the prior distribution over \vec{s} as normal random variable with mean $\vec{s}_{prior} = \frac{1}{1540 \frac{m}{s}}$ and covariance \mathbf{Q} . Rather than directly implement \mathbf{Q} as a full matrix, \mathbf{Q} is implemented implicitly as a convolution with a Gaussian blurring kernel. The Gaussian blurring kernel encodes the covariance between neighboring pixels in the slowness distribution and maintain the smoothness of the reconstruction. Maximizing the posterior likelihood results in the following least-squares reconstruction problem:

$$\min_{\vec{s}} \left\{ \frac{1}{2} (\vec{t}_{obs} - \mathbf{H}\vec{s})^T \mathbf{R}^{-1} (\vec{t}_{obs} - \mathbf{H}\vec{s}) + \frac{1}{2} (\vec{s} - \vec{s}_{prior})^T \mathbf{Q}^{-1} (\vec{s} - \vec{s}_{prior}) \right\} \quad (7)$$

The closed-form solution to this least-squares reconstruction problem is

$$\vec{s} = \vec{s}_{prior} + \mathbf{QH}^T (\mathbf{HQH}^T + \mathbf{R})^{-1} (\vec{t}_{obs} - \mathbf{H}\vec{s}_{prior}), \quad (8)$$

which can be broken into two parts

$$(\mathbf{HQH}^T + \mathbf{R})\xi = \vec{t}_{obs} - \mathbf{H}\vec{s}_{prior}, \quad (9)$$

$$\vec{s} = \vec{s}_{prior} + \mathbf{QH}^T \xi. \quad (10)$$

Equation (9) can be solved for ξ using conjugate gradient and the result is fed into (10) to update the prior slowness distribution. Note that in this form, $\vec{t}_{obs} - \mathbf{H}\vec{s}_{prior}$ is the observed phase aberration. Equations (9) and (10) summarize the implementation of IMPACT.

III. METHODS

A. Simulation of the Full Synthetic Aperture Dataset

The complete full-synthetic aperture (FSA) dataset, consisting of received channel data from individual firings from

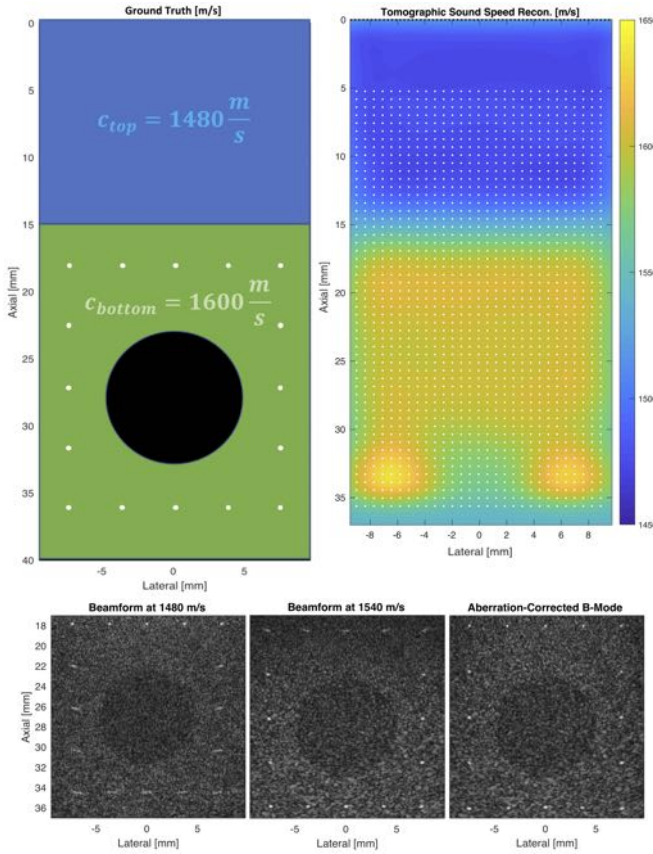


Fig. 1. Sound speed estimation and distributed aberration correction in a diffusely-scattering two-layer medium simulated in k-Wave (settings described in Table I). Resolution and lesion contrast are compared between the constant sound speed and the eikonal-corrected image formation in Table II.

each transmit element, was simulated in k-Wave [8] for a two-layer medium of random diffuse point scatterers, whose reflectivities were modified to simulate a hypoechoic lesion and surrounding point targets. The FSA dataset was also simulated for diffuse scattering in multilayered and abdominal media [9]. Each FSA dataset was then converted to I/Q channel data using the Hilbert transform. Simulation parameters such as the transducer configuration, transmit pulse, computational grid, and sampling are described in Table I.

B. Sound Speed Estimation and Image Reconstruction

FSA data were focused at all points in the ultrasound image at sound speeds ranging from 1400 to 1700 m/s. The focused, or delayed, channel data were summed across transmit channels, leaving behind receive channel data for each imaging point. Coherence factor (CF) [10], given as

$$CF = \frac{|\sum_{k=1}^N s[k]|^2}{N \sum_{k=1}^N |s[k]|^2}, \quad (11)$$

where $s[k]$ are complex samples from each of N receive channels, was measured for each imaging point and sound speed. The coherence factor images at each sound speed are spatially smoothed in order to obtain a speckle-averaged coherence

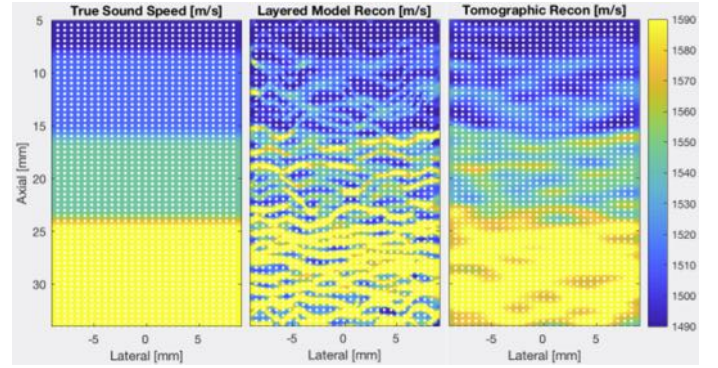


Fig. 2. Sound speed estimation in a four-layer medium

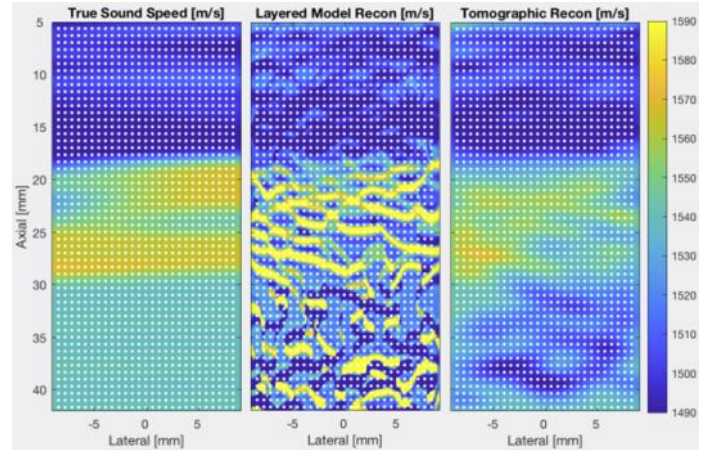


Fig. 3. Sound speed estimation in an abdominal medium

factor for each sound speed and focal point. The sound speed that maximizes CF at each focal point is determined to be the effective average speed of sound (c_{avg}). We recover estimates for the local speed of sound either by applying the layered model (equations (2) and (3)) to each vertical line down the image or the tomographic model (equations (5)-(10)) which handles all imaging points at once.

C. Travel Times in a Spatially-Varying Sound Speed Medium

Assuming a two-dimensional medium with coordinates (x, z) and sound speed $c(x, z)$ where $(x_i, 0)$ is the location of the i th element on the transducer array, the travel time τ from the i th element to an arbitrary point (x, z) in the medium can be found using the eikonal equation

$$\sqrt{\left(\frac{\partial \tau}{\partial x}\right)^2 + \left(\frac{\partial \tau}{\partial z}\right)^2} = \frac{1}{c(x, z)} \quad (12)$$

subject to the boundary condition $\tau(x_i, 0) = 0$. The eikonal equation (12) accurately models refraction and can be solved efficiently using the fast marching method [7].

IV. RESULTS

A. Sound Speed Estimation and Aberration Correction

Figure 1 shows the diagram of the medium simulated in k-Wave (simulation settings shown in Table I), the tomographic

TABLE II
 COMPARISON OF IMAGING QUALITY METRICS BETWEEN CONSTANT
 SOUND SPEED AND EIKONAL-BASED BEAMFORMING.

| | Lesion Contrast (dB) | Top Row Point Targets | | Bottom Row Point Targets | |
|-------------------------|----------------------------|--------------------------|------------|-----------------------------|------------|
| | | -6 dB | Width (mm) | -6 dB | Width (mm) |
| 1480 m/s Beamforming | 3.2012 | 0.21 | | 0.99 | |
| 1540 m/s Beamforming | 2.8817 | 0.61 | | 0.36 | |
| Eikonal | 2.8247 | 0.18 | | 0.35 | |

reconstruction of sound speed in the medium, and B-mode images based on fixed beamforming sound speeds and the aberration correction methodology based on the eikonal equation in [2]. The aberration corrected B-mode image shows that the tomographic estimate of local sound speed is accurate enough so that the resulting local sound speed distribution results in optimal focusing at all imaging points. Table II shows that aberration correction using the eikonal-based travel times leads to point target resolution that is better than the resolution achievable by constant sound speed beamforming at all depths. These results imply a strong duality between sound speed reconstruction and the focusing quality achievable by phase aberration correction: sound speed reconstruction is as accurate as the ability of phase aberration correction to improve focusing quality in the image. If small sound speed changes lead to large changes in focusing quality, sound speed should be easy to estimate accurately; conversely, if sound speed changes have a negligible effect on focusing quality, sound speed becomes difficult to estimate accurately. When applying this sensitivity analysis to the tomographic estimate, it becomes clear that focusing quality in the image is largely insensitive to sound speed variations at the deepest depths in the medium; as a result, the tomographic reconstruction has large fluctuation at the deepest imaging depths.

B. Comparing Tomographic and Layered Medium Models

In the simulated four-layer medium (Figure 2), the RMS error in local sound speed estimation improves from 47.1 m/s to 6.3 m/s when moving from the layered model to the tomographic approach. Similarly, in the simulated abdominal medium (Figure 3), the RMS error in local sound speed estimation improves from 65.4 m/s to 17.9 m/s. These improvements are due to the fact that the tomographic inversion considers all the paths leading to the focal point whereas the layered model treats each vertical line through the medium separately. However, despite these improvements, the lateral inhomogeneities in the medium are not accurately captured by the reconstruction process. Initially, in the top-most layers, tomography reasonably recovers the local sound speed distribution in the medium. However, deeper into the medium, higher order phase aberrations and errors in the assumed location of the focal points causes the local sound speed estimate to drift away from its true value. One solution to this

problem would be to focus the channel data using this estimate of the local sound speed, re-estimate phase aberration, and iterate through IMPACT until convergence is reached. Future work should investigate the convergence of this procedure and any subsequent improvements on sound speed estimation.

V. CONCLUSIONS

Previous work shows that sound speed can be measured accurately in a layered medium by relating the effective average sound speed up to a particular depth to the local sound as a function of depth. The goal of this work was to relax the requirement that medium is strictly layered by using a tomographic approach that we call IMPACT. IMPACT performs well in perfectly layered media as well as in media with moderate lateral variations in sound speed. However, IMPACT is ultimately limited by certain modeling assumptions such as perfect knowledge of the focal point. Sound speed variations can change the location of the focal point. Furthermore, our coherence-based approach does not model higher-order phase aberration. Future work should incorporate the quantification of higher-order phase aberration and investigate the convergence of an iterative IMPACT procedure that alternates between a sound speed model and the quantification of phase-aberration after focusing using the sound speed model.

ACKNOWLEDGMENT

Funding was provided by the Stanford-Philips research collaboration as well as the National Defense Science and Engineering Graduate (NDSEG) Fellowship.

REFERENCES

- [1] P. Stähli, M. Kuriakose, M. Frenz, and M. Jaeger, "Forward model for quantitative pulse-echo speed-of-sound imaging," *arXiv preprint arXiv:1902.10639*, 2019.
- [2] R. Ali and J. J. Dahl, "Distributed phase aberration correction techniques based on local sound speed estimates," in *2018 IEEE International Ultrasonics Symposium (IUS)*. IEEE, 2018, pp. 1–4.
- [3] J. F. Greenleaf and R. C. Bahn, "Clinical imaging with transmissive ultrasonic computerized tomography," *IEEE Transactions on Biomedical Engineering*, no. 2, pp. 177–185, 1981.
- [4] C. Sehgal, G. Brown, R. Bahn, and J. F. Greenleaf, "Measurement and use of acoustic nonlinearity and sound speed to estimate composition of excised livers," *Ultrasound in medicine & biology*, vol. 12, no. 11, pp. 865–874, 1986.
- [5] M. Imbault, A. Faccinetto, B.-F. Osmanski, A. Tissier, T. Deffieux, J.-L. Gennisson, V. Vilgrain, and M. Tanter, "Robust sound speed estimation for ultrasound-based hepatic steatosis assessment," *Physics in Medicine & Biology*, vol. 62, no. 9, p. 3582, 2017.
- [6] M. Jakovljevic, S. Hsieh, R. Ali, G. Chau Loo Kung, D. Hyun, and J. J. Dahl, "Local speed of sound estimation in tissue using pulse-echo ultrasound: Model-based approach," *The Journal of the Acoustical Society of America*, vol. 144, no. 1, pp. 254–266, 2018.
- [7] J. A. Sethian and A. M. Popovici, "3-d travelttime computation using the fast marching method," *Geophysics*, vol. 64, no. 2, pp. 516–523, 1999.
- [8] B. E. Treeby and B. T. Cox, "k-wave: Matlab toolbox for the simulation and reconstruction of photoacoustic wave fields," *Journal of biomedical optics*, vol. 15, no. 2, p. 021314, 2010.
- [9] T. D. Mast, L. M. Hinkelman, M. J. Orr, V. W. Sparrow, and R. C. Waag, "Simulation of ultrasonic pulse propagation through the abdominal wall," *The Journal of the Acoustical Society of America*, vol. 102, no. 2, pp. 1177–1190, 1997.
- [10] R. Mallart and M. Fink, "Adaptive focusing in scattering media through sound-speed inhomogeneities: The van cittert zernike approach and focusing criterion," *The Journal of the Acoustical Society of America*, vol. 96, no. 6, pp. 3721–3732, 1994.